# TOPOLOGICAL CHARACTERISTICS OF 5D SPATIALLY DYNAMIC BRAIN NETWORKS IN SCHIZOPHRENIA

Mustafa S. Salman<sup>⋆†</sup>

Armin Iraji<sup>†</sup>

Noah Lewis<sup>†‡</sup>

Vince D. Calhoun<sup>⋆†</sup>

\* School of Electrical and Computer Engineering, Georgia Institute of Technology

† Tri-institutional Center for Translational Research in Neuroimaging & Data Science (TReNDS),
Georgia Institute of Technology, Georgia State University, & Emory University

‡ School of Computational Science and Engineering, Georgia Institute of Technology
Atlanta, GA, USA

#### **ABSTRACT**

The last decade of rich data-driven research on functional magnetic resonance imaging (fMRI) has provided novel insights into human brain function and aberrant behavior in brain disorders. Independent component analysis (ICA) is a widely-used technique for data-driven analysis of fMRI data. Spatial ICA is the most prominent variation of ICA and provides replicable and interpretable intrinsic connectivity network (ICN). It assumes common spatial activation across time. However, very recent studies indicate that there is utility in adopting a dynamic spatial activation modeling approach. Characterizing dynamics for both temporal and spatial domains means we have a multitude of decompositions of the already high-dimensional, multi-dataset, and multi-subject fMRI data. Hence making sense of the derived data becomes a significant issue. Here we use topological data analysis (TDA) to identify topological descriptors of the windowed spatially dynamic components of fMRI data. We discover and summarize differences in the spatial dynamics of controls and schizophrenia patients (SZs). We discover that SZs generally have lower Betti numbers and higher Wasserstein distance between spatiotemporal brain states, which provide intuitive summaries of the reduced dynamism SZs exhibit in resting-state fMRI studies.

*Index Terms*— fMRI, brain dynamics, spatial dynamics, schizophrenia, topological data analysis, Betti number, Wasserstein distance

## 1. INTRODUCTION

fMRI is a noninvasive imaging method extensively used to study human brain function. Seed-based and data-driven approaches are two widely used methods of analyzing fMRI data. Group ICA is a popular data-driven method for multisubject fMRI studies [1]. In this method, the spatial ICA algorithm decomposes the data into a linear combination of spatially and statistically independent components (ICs) and

associated time courses (TCs). The coherence of TCs from distant brain regions, or networks, show functionally synchronized low-frequency blood-oxygen-level-dependent (BOLD) activity [2, 3] This synchronism is referred to as functional network connectivity (FNC) or dynamic functional network connectivity (dFNC) when resolved into time windows [4].

Recent studies by Iraji et al. challenge the assumption of the static nature of the brain networks and show that these vary spatially in time at the voxel level [5]. By focusing on the variation of networks coupling at the voxel level, the authors reveal features that are spatially dynamic, and brain networks that transiently integrate and segregate.

Topological data analysis (TDA) is an emerging field motivated by the application of algebraic topology and computational geometry to complex data analysis [6]. The goal is to build higher-dimensional generalizations of neighboring graphs on the data. This can be done via proposed mathematical theories and computational tools for analysis, with many recent promising and successful results in many fields.

In this work, we ask how dynamic the resting-state brain networks in the human brain are in the spatial domain. We turn to TDA for some concise and objective answers. Fig. 1 shows a simple overview of the analysis. We reduce the temporally evolving brain networks into a few tractable brain states. We then quantify the topological descriptors of those states, specifically state Betti numbers and Wasserstein distance between the state pairs.

#### 2. METHODS

## 2.1. Data

We used resting-state fMRI data from three datasets in this study: Function Biomedical Informatics Research Network (FBIRN), Centers of Biomedical Research Excellence (COBRE) and Maryland Psychiatric Research Center (MPRC). The population information and acquisition parameters of each dataset are listed in Table. 1.

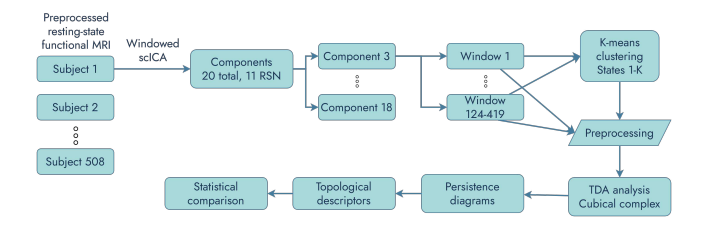


**Fig. 1:** Flowchart of the analysis. 11 resting state networks (RSNs) were estimated from each time window (of duration 30 TR) of the preprocessed fMRI data of each subject. k-means clustering (k=4) was used to label each windowed intrinsic connectivity network (ICN), and each cluster's mean network/state was estimated. The mean state spatial maps (SMs) were put through TDA analysis, and the topological descriptors were calculated. Finally, statistical comparisons between controls and patients were made on the descriptors.

## 2.2. Preprocessing

We used Statistical Parametric Mapping (SPM) (https://www.fil.ion.ucl.ac.uk/spm/) and Analysis of Functional NeuroImages (AFNI) (https://afni.nimh.nih.gov/) to preprocess the raw fMRI data. We performed the following steps as part of preprocessing: brain extraction, motion correction using the INRIAlign toolbox, slice-timing correction using the middle slice as a reference, despiking using AFNI 3dDespike tool, warping to the Montreal Neurological Institute (MNI) template, resampling to  $3mm^3$  isotropic voxels, spatial smoothing using a Gaussian kernel with 6mm full width at half maximum (FWHM), and variance-normalization (z-scoring) each voxel time course.

# 2.3. Group-level Network Estimation

We estimated the group-level brain networks from the preprocessed data using the group spatial ICA approach [1]. For this purpose, we used the Group ICA of fMRI Toolbox (GIFT) software (https://trendscenter.org/software/gift/) [7]. We re-

**Table 1**: Population information & acquisition parameters

Dataset	FBIRN	COBRE	MPRC
Population info			
Controls	88	75	152
Schizophrenia patients	60	51	82
Total	148	126	234
Mean age	37.59	38.09	39.26
S.D. of age	10.88	13.27	13.92
Acquisition parameters			(3 sites)
Scanner type	Siemens 3 T	Siemens 3 T	Siemens 3 T
TR	2 sec.	2 sec.	2/2.21/2 sec.
TE	30 ms	29 ms	27/30/30 ms
Slices	32	33	
Slice thickness	4 mm	3.5  mm	
Slice gap	1 mm	1.05  mm	
Flip angle	77	75°°	
FOV	$220mm^2$	$240mm^2$	$220mm^2$
Matrix size	$64 \times 64$	$64 \times 64$	
Scan duration	5 min.	5 min.	
Volumes	162	149	150/140/444

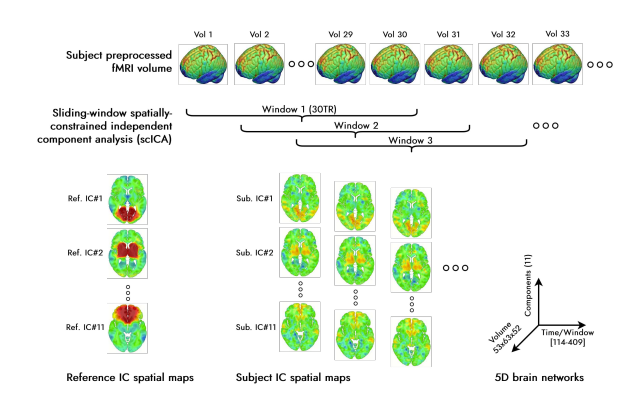


**Fig. 2:** Spatially dynamic windowed ICN estimation. Spatially constrained ICA (scICA) algorithm was applied to each subject's fMRI volumes in sliding windows of duration 30 TR. Resultant components show spatio-temporal variation in the 5-dimensional space.

duced the preprocessed fMRI data a subject-level principal component analysis (PCA), followed by a group-level PCA, and finally an ICA step to identify the spatial independent components (ICs) using the infomax algorithm [8]. We used a low model order ICA to estimate 20 group-level ICs to limit the number of group comparison, although higher model order . We identified 11 RSNs from these ICs using their spatial and temporal properties and our prior knowledge of brain anatomy and function [4].

#### 2.4. Spatially Dynamic Network Estimation

We used a sliding window approach and the group informationguided ICA (GIG-ICA) framework to estimate the spatially dynamic brain networks for each subject. This constrained ICA based approach has been proven to be robust in fMRIbased group analyses [9]. Fig. 2 shows how this approach was implemented. In the sliding window approach, we took the preprocessed subject fMRI data and applied sliding windows of size 30TR on it, with a step size of 1TR. At each window, we estimated the ICs of the subject using the GIG-ICA approach. This approach allows us to estimate corresponding networks at each window and thus observe the spatial alternations in such networks. GIG-ICA computes the ICs of individual subjects by re-optimizing the independence among them while still preserving the correspondence of networks across subjects [10]. This results in greater independence of components and improved accuracy of the ICs and TCs.

## 2.5. Spatial States of Brain Networks

Spatial dynamics operates in a large space in this dataset. So we used k-means clustering to reduce the dimension of the data along the time/window dimension. For each windowed ICN, we applied k-means clustering on a total of 78374 windows across 508 subjects. We implemented the k-means clus-

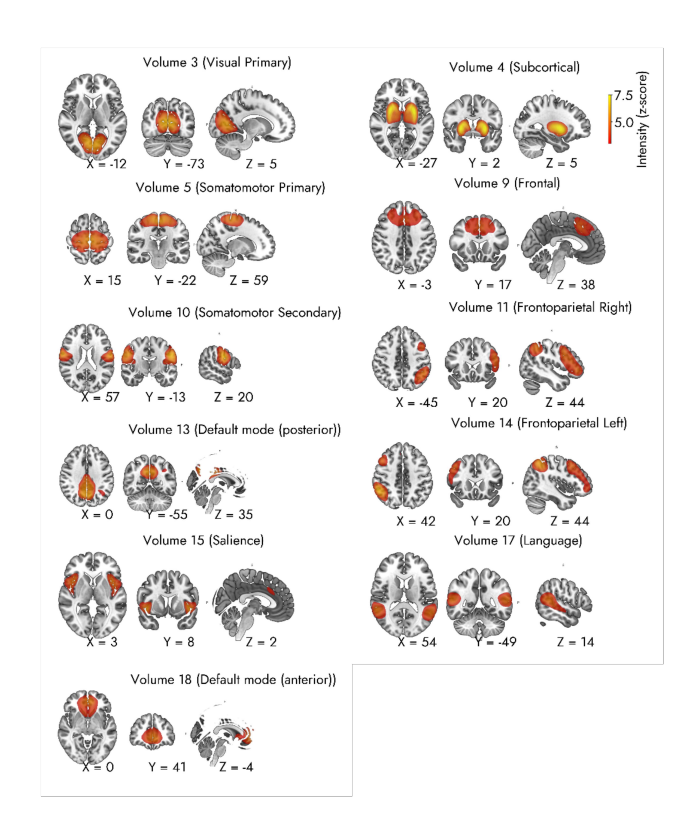


Fig. 3: Group-level reference networks used for feature extraction in the scICA step

tering using python scikit-learn package with k=4 and 10 replicates. To justify the choice of k, we evaluated k-means clustering using a range of k between [3-8] and found that for most of the ICs, k=4 minimized the Davis-Bouldin criterion [11].

## 2.6. Topological Data Analysis

TDA of spatially dynamic networks involves estimating three steps from every state of the windowed ICN for each subject: 1. cubical complex, 2. filtration, and 3. persistence diagrams. We performed the TDA analysis using the Python GUDHI toolbox (https://gudhi.inria.fr/). An fMRI volume is already preprocessed into a grid of dimensions  $53 \times 63 \times 52$ . Therefore, the conversion to the cubical complex is straightforward [12]. Each vertex of the cubical complex is a voxel in the fMRI volume. The regular 3D grid defines the edges between the vertices, and each vertex has six neighbors. These neighborhoods define the higher-dimensional elements of the cubical complex, such as squares and cubes. Low-dimensional topological features such as Betti numbers arise as a result. 0-dimensional, 1-dimensional, and 2-dimensional topological features are known as connected components, "circular" holes, and "voids" or "cavities", respectively. In this work, we looked at the Betti number of 1-dimensional holes  $(b_1)$  in the windowed ICNs as a potentially informative topological

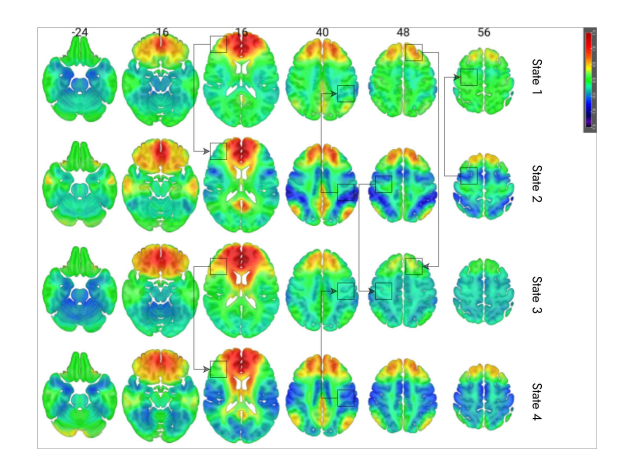


Fig. 4: The 4 spatially dynamic states of the IC#18 (anterior default mode network) across subjects/time windows. The connected square blocks indicate some of the regional differences in intensity of different states of the same ICN across subjects.

descriptor. We also transformed the voxel intensities to absolute values and thresholded them at the intensity value of 1. The voxel intensity values can be treated as the activation function that allows us to apply filtration on the cubical complex. Topological features such as connected components are created and destroyed at various levels of filtration. Finally, the persistence diagram summarizes the topological activities at level of filtration. Wasserstein distance measures the similarity between two persistence diagram and it is the other metric of interest in our work.

#### 2.7. Statistical Comparison

We intended to compare two metrics: state-wise Betti numbers in 1-dimension and Wasserstein distance between each state pair for each windowed ICN between the two groups, controls and SZ. For this purpose, we first regressed out the effect of age and gender variables on the above metrics using ordinary least squares regression. The residuals had a right-tailed distribution. Next we examined the effect of the diagnosis variable on the log residuals of the models using a two-sample T-test.

#### 3. RESULTS

Fig. 3 shows the 11 group-level networks estimated from the data. These are labeled according to their function based on prior knowledge. Fig. 4 shows each cluster or spatial state mean across all subjects from one windowed ICN (IC#3, visual primary). Here we show the four spatial states of the same IC, demonstrating considerable spatial variation in time.

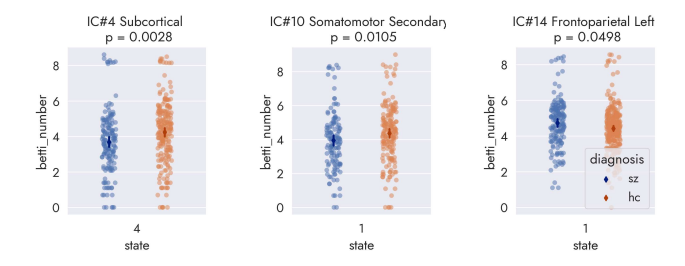


**Fig. 5**: Difference in log Betti numbers in 1-dimension between controls and SZ. The three instances where a significant difference was observed are shown. Solid dots and lines indicate mean and 95% CI respectively. SZ generally has higher Betti numbers than controls, indicating more holes in the IC topology.

## 3.1. Group Difference in Betti Numbers

In total, across all IC/state combinations, we made a total of 43 comparisons in the log Betti numbers in 1-dimension between controls and SZ. Note that for some IC/state combinations, some subjects may not have any data because they do not spend any time in that state. Moreover, for different ICN the experiments are independent. SZs show lower Betti numbers in 1-dimension compared to controls in 15 of the 43 experiments. The three instances where a significant difference was observed are shown in Fig. 5. Solid dots and lines indicate mean and 95% confidence interval respectively. The significant differences are located in subcortical, secondary somatomotor and left frontoparietal regions. SZ generally has lower Betti numbers than controls, indicating a lower number of holes in the IC topology of the patients. We do not correct the p-values for multiple comparisons because the number of experiments is small enough for each ICN.

## 3.2. Group Difference in Wasserstein Distance

Across all IC/state combinations, we made a total of 63 comparisons in the log Wasserstein distance between state windowed ICN pairs between controls and SZ. Similar to the experiments with Betti numbers, some subjects may not have any data for a particular IC/state-pair combination. SZs show higher Wasserstein distance than controls in 36 of the 63 experiments. The eight instances where a significant difference was observed are shown in Fig. 6. Three of the differences are observed in the left and right frontoparietal regions, two in the visual primary region, and the rest are in the salience, language and anterior default mode networks. SZ generally has higher pairwise Wasserstein distance than controls, indicating reduced dynamism in the spatial dynamic space.

## 4. DISCUSSION

Recent work highlights the importance of studying brain spatial dynamics to understand brain function [13]. In this work,

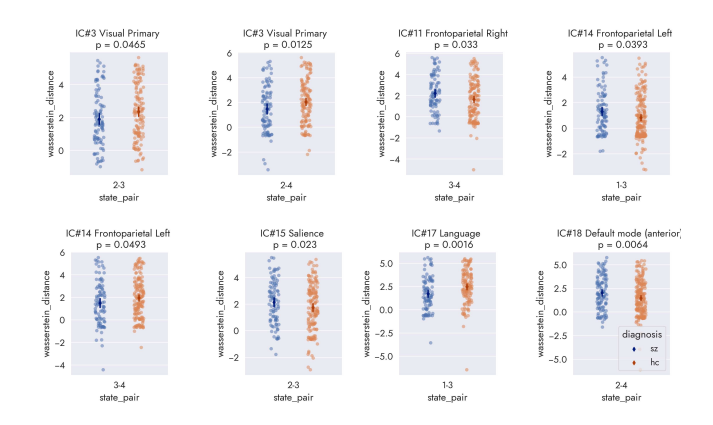


Fig. 6: Difference in log pairwise Wasserstein distance between states between controls and SZ. The eight instances where a significant difference was observed are shown. Solid dots and lines indicate mean and 95% CI respectively. SZ generally has a higher Wasserstein distance than controls.

we used TDA to develop novel summary metrics to express brain function in the spatial dynamics space. We found distinct topological descriptors in the windowed ICNs of SZs that discriminate them from the controls. Considering the number of windowed ICN and state or state-pair combination, we saw that patients generally have lower Betti numbers in 1-dimension and higher Wasserstein distance between state-pairs in the windowed ICN. Increased Betti number in 1-dimension indicates the presence of more "circular holes" in the IC maps of the controls. Wasserstein distance is also known as "earth mover's distance" or "optimal transport cost." Our results indicate that it incurs a higher cost for SZs to switch brain states in the spatial dynamic space. When we put our findings in light of previous literature [14, 15], it can explain the reason for reduced dynamism in SZ in terms of the topological properties of the brain networks.

Spatial dynamics is a novel approach to understanding brain function using resting-state fMRI, and our work is the first TDA-based approach in this space. As such, our work has both limitations and many promising future directions. The cubical complex transformation can be improved with some preprocessing steps. It can be helpful to min-max scale the voxel intensities between values [0-1], and then apply sub-level set filtration on the complement of the intensity values because it can result in more meaningful Betti numbers. We used k-means clustering for identifying the spatially dynamic brain states. However, a topological clustering method based on the Wasserstein distance matrix between pair-wise volumes can be more helpful. Future work may focus on the trajectory of the persistence diagrams across time windows and applying a different complex function on the brain surface.

#### 5. COMPLIANCE WITH ETHICAL STANDARDS

Informed consent was obtained from the participants according to the guidelines set by the Internal Review Boards at the sites of each study (FBIRN, COBRE, and MPRC).

#### 6. ACKNOWLEDGEMENT

This work was supported by the National Institutes of Health grant R01MH123610 and the National Science Foundation grant 2112455 (to Calhoun VD).

#### 7. REFERENCES

- V.D. Calhoun, T. Adali, G.D. Pearlson, and J.J. Pekar, "A method for making group inferences from functional MRI data using independent component analysis," *Human Brain Mapping*, vol. 14, no. 3, pp. 140– 151, Nov. 2001.
- [2] Michael D. Greicius, Ben Krasnow, Allan L. Reiss, and Vinod Menon, "Functional connectivity in the resting brain: A network analysis of the default mode hypothesis," *Proc. Natl. Acad. Sci. U.S.A.*, vol. 100, no. 1, pp. 253–258, Jan. 2003.
- [3] Bharat Biswal, F. Zerrin Yetkin, Victor M. Haughton, and James S. Hyde, "Functional connectivity in the motor cortex of resting human brain using echo-planar mri," *Magnetic Resonance in Medicine*, vol. 34, no. 4, pp. 537–541, Oct. 1995.
- [4] E. A. Allen, E. Damaraju, S. M. Plis, E. B. Erhardt, T. Eichele, and V. D. Calhoun, "Tracking Whole-Brain Connectivity Dynamics in the Resting State," *Cerebral Cortex*, vol. 24, no. 3, pp. 663–676, Mar. 2014.
- [5] Armin Iraji, Thomas P. Deramus, Noah Lewis, Maziar Yaesoubi, Julia M. Stephen, Erik Erhardt, Aysneil Belger, Judith M. Ford, Sarah McEwen, Daniel H. Mathalon, Bryon A. Mueller, Godfrey D. Pearlson, Steven G. Potkin, Adrian Preda, Jessica A. Turner, Jatin G. Vaidya, Theo G. M. van Erp, and Vince D. Calhoun, "The spatial chronnectome reveals a dynamic interplay between functional segregation and integration," *Human Brain Mapping*, vol. 40, no. 10, pp. 3058–3077, July 2019.

- [6] Gunnar Carlsson, "Topology and data," Bull. Amer. Math. Soc., vol. 46, no. 2, pp. 255–308, 2009.
- [7] Armin Iraji, Ashkan Faghiri, Noah Lewis, Zening Fu, Srinivas Rachakonda, and Vince D Calhoun, "Tools of the trade: Estimating time-varying connectivity patterns from fMRI data," *Social Cognitive* and Affective Neuroscience, p. nsaa114, Aug. 2020.
- [8] Anthony J. Bell and Terrence J. Sejnowski, "An Information-Maximization Approach to Blind Separation and Blind Deconvolution," *Neural Computation*, vol. 7, no. 6, pp. 1129–1159, Nov. 1995.
- [9] Marlena Duda, Armin Iraji, and Vince D. Calhoun, "Spatially Constrained ICA Enables Robust Detection of Schizophrenia from Very Short Resting-state fMRI," in 2022 44th Annual International Conference of the IEEE Engineering in Medicine & Biology Society (EMBC), July 2022, pp. 1867–1870.
- [10] Yuhui Du and Yong Fan, "Group information guided ICA for fMRI data analysis," *NeuroImage*, vol. 69, pp. 157–197, Apr. 2013.
- [11] D. L. Davies and D. W. Bouldin, "A Cluster Separation Measure," IEEE Transactions on Pattern Analysis and Machine Intelligence, vol. PAMI-1, no. 2, pp. 224–227, Apr. 1979.
- [12] Bastian Rieck, Tristan Yates, Christian Bock, Karsten Borgwardt, Guy Wolf, Nicholas Turk-Browne, and Smita Krishnaswamy, "Uncovering the Topology of Time-Varying fMRI Data using Cubical Persistence," p. 13.
- [13] Armin Iraji, Robyn Miller, Tulay Adali, and Vince D. Calhoun, "Space: A Missing Piece of the Dynamic Puzzle," *Trends in Cognitive Sciences*, vol. 24, no. 2, pp. 135–149, Feb. 2020.
- [14] E. Damaraju, E.A. Allen, A. Belger, J.M. Ford, S. McEwen, D.H. Mathalon, B.A. Mueller, G.D. Pearlson, S.G. Potkin, A. Preda, J.A. Turner, J.G. Vaidya, T.G. van Erp, and V.D. Calhoun, "Dynamic functional connectivity analysis reveals transient states of dysconnectivity in schizophrenia," *NeuroImage: Clinical*, vol. 5, pp. 298–308, 2014.
- [15] Robyn L. Miller, Maziar Yaesoubi, Jessica A. Turner, Daniel Mathalon, Adrian Preda, Godfrey Pearlson, Tulay Adali, and Vince D. Calhoun, "Higher Dimensional Meta-State Analysis Reveals Reduced Resting fMRI Connectivity Dynamism in Schizophrenia Patients," *PLOS ONE*, vol. 11, no. 3, pp. e0149849, Mar. 2016.